ELSEVIER

Journal of Electroanalytical Chemistry 397 (1995) 119–126

JOURNAL OF ELECTROANALYTICAL CHEMISTRY

Toward molecular selectivity with chemically modified electrodes: can electroactivity and permeability through an overlaying metallopolymer film be controlled via rational manipulation of internal architecture?

Susan G. Yan, Joseph T. Hupp *

Department of Chemistry and Materials Research Center, Northwestern University, Evanston, IL 60208, USA

Received 29 November 1994; in revised form 5 May 1995

Abstract

Metallopolymeric films featuring widely varying metal-to-metal linkage lengths have been prepared via a combination of oxidative and reductive electropolymerization schemes. Each of the film materials exhibits strong size selective permeability behavior towards molecular reactants, therefore providing a primitive physical basis for selectivity with respect to reactivity at an underlying electrode. Surprisingly, the observed molecular size cut-offs are essentially independent of film composition, implying that a uniform molecular cavity or pore size exists. Attempts to modify effective pore sizes by introducing large ligand substituents (phenyl groups) at the monomer synthesis stage have failed to alter the pattern of size selectivity. We speculate that (a) potential pore size expansion effects expected from linkage length extension are offset by enhanced cross-linking, and/or (b) electrolyte anion templating effects during film synthesis may be defining the effective minimum pore size, thereby yielding uniform permeation size cut-offs.

Keywords: Molecular structure; Film structure; Molecular selectivity; Chemically modified electrodes; Electroactivity; Permeability; Metallopolymer film

1. Introduction

One of the objectives of chemical modification of electrode surfaces, particularly for electrocatalytic and sensing applications, is to impart molecular selectivity. Among the simplest approaches to achieving selectivity would be discrimination on the basis of physical size. Indeed, several reports exist wherein size selectivity or "molecular sieving" is achieved via permeation through (or exclusion by) a polymer film containing pores or cavities of a particular molecular size (or size range) [1–7]. We reasoned that selectivity could be systematically tuned if (a) linkage lengths (and presumably, therefore, cavity dimensions) in a cross-linked polymer could be systematically varied and/or (b) monomer substituent sizes (and presumably, therefore, effective cavity volumes) in the same or similar polymers could likewise be varied. We report here the results of our efforts to control selectivity via both strategies.

The system selected was a metallopolymer coating on platinum with primarily ferrocene species as permeants. The particular choice of polymer was one derived from ruthenium complexes of 1,10-phenanthroline (phen) and any of several bipyridines, where one of the nitrogens of each of two bipyridine ligands (L) remains uncoordinated in the monomeric compound. We have previously shown that these complexes polymerize rapidly following electrochemical oxidation of the metal center [8,9] (for a related report, see Calvert et al. [10]). When the oxidation is carried out by cyclic voltammetry, adherent electrode film coatings are obtained that retain the electrochemical properties of the monomeric precursors. The mechanism of polymerization appears to involve nucleophilic attack of phenanthroline by the free pyridyl nitrogen, where attack is activated by ruthenium oxidation. In any case, crystallographic studies of related monomeric reaction products

* Corresponding author.

SSDI 0022-0728(95)04176-1

(unpublished) have established that the linkage structure (for L = 4,4′-bipyridine) is the following [11]:

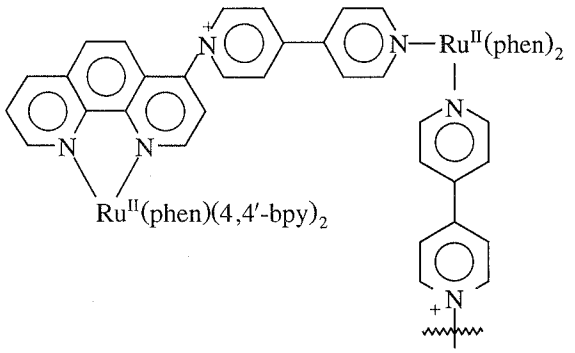

We reasoned that linkage lengths could be manipulated arbitrarily by replacing 4,4′-bipyridine with ligands featuring hydrocarbon spacers between the pyridyl rings. Alternatively, metallopolymers featuring shorter linkages of a slightly different form can be obtained via oxidative or reductive activation respectively of Fe(5-amino-1,10-phenanthroline)$_3^{2+}$ [12] or Ru(5-chloro-1,10-phenanthroline)$_3^{2+}$ [13], as shown below:

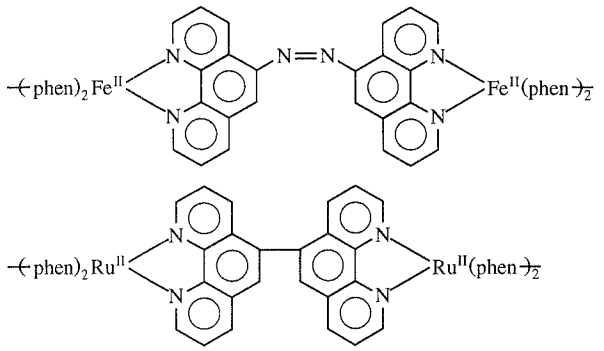

Finally, we reasoned that, with electroactive permeants such as ferrocene, permeation (and therefore selectivity) could be assessed quantitatively by monitoring transient and steady state oxidation currents at the underlying electrode, as in previous investigations [1–7].

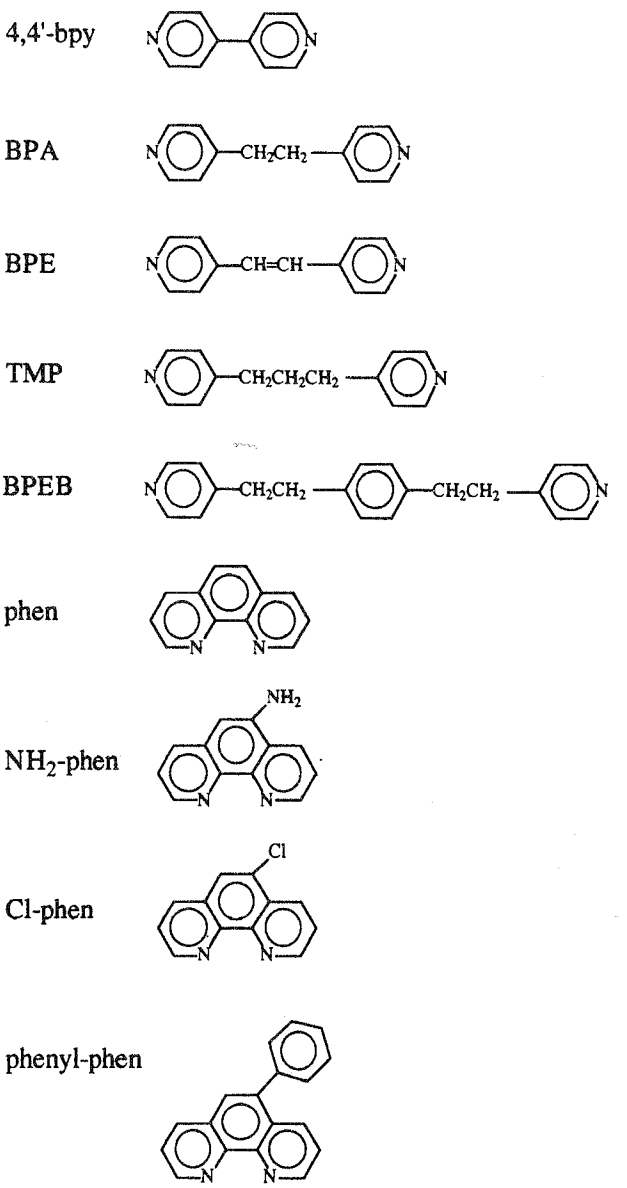

Fig. 1. Ligand structures and abbreviations.

2. Experimental

2.1. Materials

$RuCl_3$ was purchased from Aesar. 1,10-Phenanthroline, 5-chloro-1,10-phenanthroline (Cl-phen) and 5-phenyl-1,10-phenanthroline (phenyl-phen) were purchased from GFS Chemicals. (Ligand structures are shown in Fig. 1.) 5-Amino-1,10-phenanthroline (NH_2-phen) was purchased from Polysciences. 4,4′-Bipyridine (4,4′-bpy), 1,2-bis(4-pyridyl)ethylene (BPE), 1,2-bis(4-pyridyl)ethane (BPA) and 4,4′-trimethylenedipyridine (TMP) were purchased from Aldrich Chemical Co. Reagent grade acetonitrile and dichloromethane were purchased from Fisher and distilled from CaH_2 prior to use. Tetrabutylammonium perchlorate (TBAP) (GFS Chemicals) was recrystallized in purified distilled water and dried in a vacuum.

β,β′-bis(4-pyridyl)-1,4-diethylbenzene (BPEB) was prepared as follows. Lithium diispropylamide (0.0103 mol), prepared from diisopropylamine and butyllithium in 10 ml distilled tetrahydrofuran (THF) under N_2, was added dropwise to 1.0 ml distilled 4-picoline in 100 ml THF in an acetone + dry ice bath and stirred for 20 min. α,α′-Dibromo-*p*-xylene (1.36 g (5.15×10^{-3} mol)), purified by recrystallization from hot methanol, was dissolved in 50 ml THF and added dropwise to the orange 4-picoline solution. The mixture was stirred overnight under N_2, whereupon it turned light pink, and then 100 ml of NaCl + H_2O was added. THF was evaporated and a tan compound precipitated. This material (crude product) was then removed by extraction into distilled dichloromethane. After

evaporation of the dichloromethane, a yellow semicrystalline residue was collected. The residue was purified by recrystallization from ethyl acetate. Calculated (found) analysis: C, 82.86 (83.30); H, 7.23 (6.99); N, 9.60 (9.71). ^{1}H NMR ($CDCl_3$): d 8.5 (4H), 7.06 (8H), 2.9 (8H). Mass spectrometry: $m/e = 287$, 196, 104.

2.2. Permeants

Several ferrocene species were purchased from the Aldrich Chemical Co. (either Aldrich's standard catalog listing or the Sigma–Aldrich Library of Rare Chemicals). $Fe(vbpy)_2(CN)_2$ was synthesized via literature methods [14,15]. The structures of the permeants are shown in Fig. 2.

2.3. Polymer precursors

$[Fe(NH_2\text{-phen})_3](PF_6)_2$ and $[Ru(Cl\text{-phen})_3](PF_6)_2$ were prepared by published methods [12,13]. The various $[Ru(5\text{-R-phen})_2L_2](PF_6)_2$ (R = H or phenyl; L = 4,4′-bpy, BPE, BPA, TMP or BPEB) species were prepared and purified by a general literature method [16]. Several of these compounds have been reported previously [8,9]. For new compounds the following elemental analysis data were obtained. Calculated (found) analysis for $[Ru(phen)_2$-

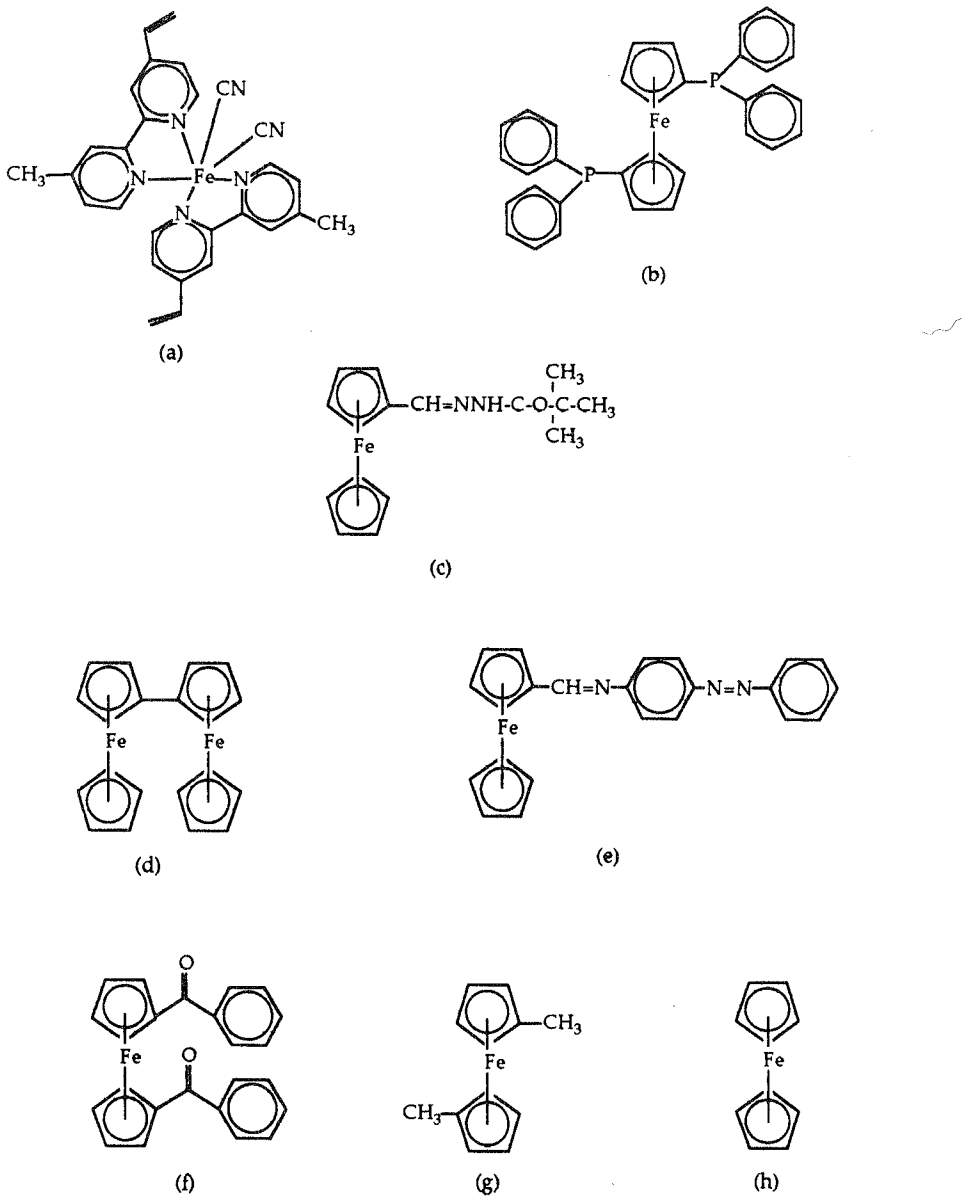

Fig. 2. Permeant structures: (a) $Fe(vbpy)_2(CN)_2$; (b) 1,1′-bis(diphenylphosphino)ferrocene; (c) *t*-butyl-3-ferrocenylmethylene carbazate; (d) 1,1′-biferrocene, (e) N-ferrocenemethylene-4-phenylazo aniline; (f) 1,1′-dibenzoylferrocene; (g) 1,1′-dimethylferrocene; (h) ferrocene.

$(BPEB)_2](PF_6)_2$: C, 55.34 (57.88); H, 4.29 (4.25); N, 7.75 (8.44). Calculated (found) analysis for [Ru(5-phenyl-phen)$_2$4-(4,4′-4-bpy)$_2$]$(PF_6)_2 \cdot H_2O$: C, 54.60 (54.51); H, 3.40 (3.43); N, 8.77 (9.08). Calculated (found) analysis for [Ru(5-phenyl-phen)$_2$(TMP)$_2$]$(PF_6)_2 \cdot 3H_2O$: C, 54.57 (54.01); H, 4.00 (3.99); N, 8.36 (8.54).

2.4. Measurements

Cyclic voltammetry measurements were made using a Princeton Applied Research polarographic analyzer (model 264A) and a Houston Instruments x–y recorder (model 2000). For rotating-disk electrode (RDE) measurements a Pine Instruments analytical rotator (model MSRX) was also employed. Electrochemical measurements were made in standard two-compartment cells containing 0.1 M TBAP in acetonitrile, or occasionally dichloromethane (see below), as solvent. The cells featured a platinum disk working electrode (1 mm diameter), a platinum wire counter-electrode and a saturated (sodium chloride) calomel reference electrode (SSCE).

3. Results and discussion

3.1. Metallopolymer synthesis

As suggested by the growth cycles in Fig. 3, adherent films of poly-Ru(phen)$_2$L$_2^{n+}$ were readily prepared from ca. 1 mM solutions of monomer via repetitive voltammetry (100 mV s^{-1}) between 0.70 and 1.70 V (i.e. the Ru(II/III) region). For Ru(phen)$_2$(4,4′-bpy)$_2^{2+}$, Ru(phen)$_2$(BPA)$_2^{2+}$, Ru(phen)$_2$(BPE)$_2^{2+}$ and Ru(phen)$_2$(TMP)$_2^{2+}$, films proved accessible from acetonitrile as the polymerization medium. For Ru(phen)$_2$(BPEB)$_2^{2+}$, Ru(5-phenyl-phen)$_2$(4,4′-bpy)$_2^{2+}$ and Ru(5-phenyl-phen)$_2$(TMP)$_2^{2+}$, however, polymeric films were obtained only from dichloromethane. Independent of the medium for polymerization, the series of films uniformly exhibited stable metal-centered electrochemical responses in monomer-free solutions. Therefore film thicknesses could be estimated by integrating the responses and utilizing Faraday's law. (Effective monomer dimensions of ca. 15 Å × 15 Å × 15 Å were assumed in thickness calculations. Calculated metal-to-metal separation distances through fully extended linkages range from 11 to 23 Å.)

3.2. Permeation: general studies

Fig. 4 shows representative voltammograms for ferrocene and dibenzoylferrocene containing solutions at bare (top panel) and poly-Ru(phen)$_2$(TMP)$_2^{n+}$-coated (bottom panel) electrodes (stationary electrodes). The comparison clearly shows that the polymer-coated electrode selectively responds to ferrocene, the smaller of the two reactants. Additionally, the response at the coated electrode is distorted in a manner that is strongly suggestive of mass transport inhibition by slow diffusion (permeation) through a barrier layer (i.e. the metallopolymer).

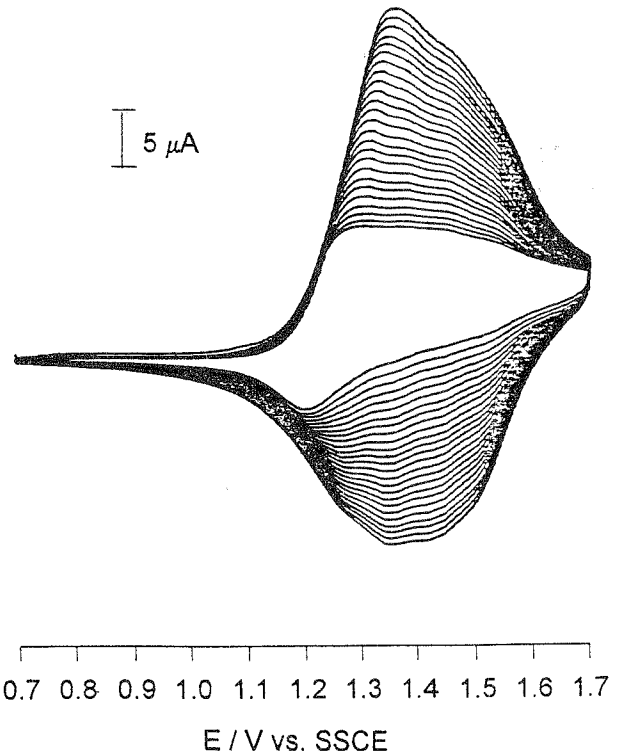

Fig. 3. Consecutive voltammograms (100 mV s^{-1}) for oxidative growth of a poly-Ru(phen)$_2$(TMP)$_2^{n+}$ film on a 1 mm diameter platinum disk in acetonitrile.

To place the studies on a more quantitative basis, we employed RDE voltammetry. Under these conditions, the limiting rate (or current I_{lim}) for solute oxidation necessarily depends on both the rate of mass transport (forced convection) through the solution phase and the rate of permeation through the polymer film. If these are viewed as consecutive rate processes, then [4]

$$I_{lim}^{-1} = I_{\text{mass transport}}^{-1} + I_{\text{permeation}}^{-1} \quad (1)$$

The individual terms are further defined as [4]

$$I_{\text{mass transport}} = 0.620nFAD^{2/3}\omega^{1/2}\nu^{-1/6}c_{soln} \quad (2)$$

$$I_{\text{permeation}} = nFAPD_{film}c_{soln}/d \quad (3)$$

where ω is the rotation rate, ν is the kinematic viscosity, n is the number of electrons transferred per permeant, F is the Faraday constant, A is the electrode area, c_{soln} is the solute concentration and d is the polymer film thickness. The permeability PD_{film} is the product of the solute partition coefficient P and its diffusion coefficient D_{film} within the film.

As suggested by Eqs. (1)–(3), the effects of convection and permeation can be separated by measuring the overall rate of solute oxidation as a function of electrode rotation rate. Fig. 5 shows a plot of I_{lim}^{-1} versus $\omega^{-1/2}$ for ferrocene oxidation at a poly-Ru(phen)$_2$(TMP)$_2^{n+}$-coated

electrode. From the intercept, $I_{permeation}$ is 19 μA and PD_{film} is 2.1×10^{-8} cm^2 s^{-1}. An additional experiment in which $I_{permeation}$ was measured as a function of inverse film thickness (Fig. 6; Eq. (3)) confirms that film-based transport does indeed occur by permeation rather than, for example, pinhole diffusion. (Other experiments established that (a) the plots varied, as expected, with changes in ferrocene concentration and (b) solution-phase diffusion coefficients determined from slopes of I_{lim}^{-1} versus $\omega^{-1/2}$ for film-covered electrodes matched those obtained at base electrodes.)

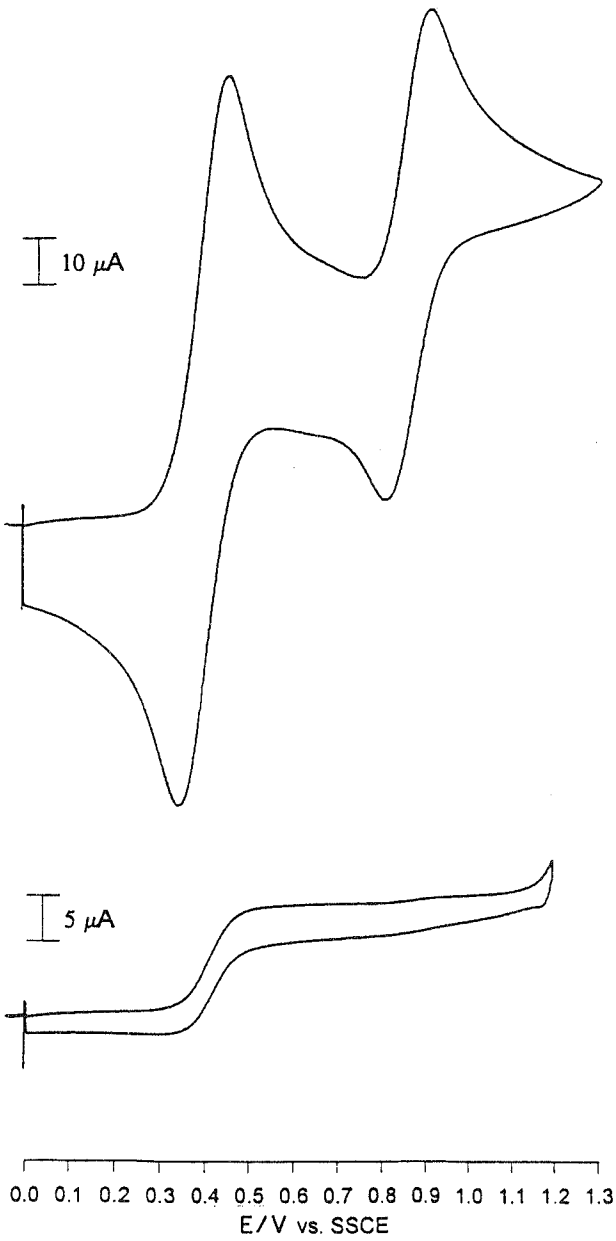

Fig. 4. Stationary voltammograms (100 mV s^{-1}) for an acetonitrile solution containing 1 mM ferrocene ($E_f = 400$ mV) and 1 mM dibenzoylferrocene ($E_f = 880$ mV): (A) bare platinum electrode; (B) poly-Ru(phen)$_2$(TMP)$_2^{n+}$-coated platinum electrode (film thickness, ca. 3×10^{-6} cm; film coverage, ca. 2×10^{-9} mol cm^{-2}).

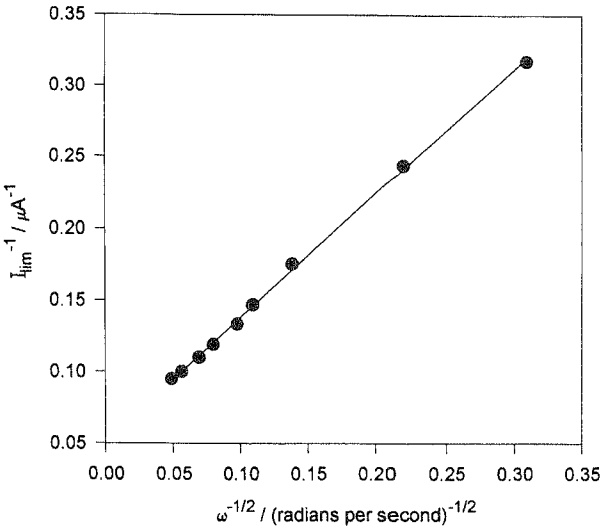

Fig. 5. Rotating-disk voltammetry: I_{lim}^{-1} versus $\omega^{-1/2}$ for oxidation of ferrocene (1 mM) at a poly-Ru(phen)$_2$(TMP)$_2^{n+}$-coated electrode (coverage, ca. 8×10^{-9} mol cm^{-2}).

3.3. Permeant dependence

To explore the issue of selectivity — especially molecular sieving — we also examined permeation as a function of permeant size. To avoid complications from either electrostatic enhancement of partitioning or Donnan exclusion, we limited our study to neutral permeants. As indicated by Fig. 2, the majority of the permeants were ferrocene species, where size variations were achieved by varying the identities and therefore the sizes of substituents. However, because many of the permeants are irregularly shaped, a fully satisfactory description of relative sizes was difficult to establish. Ultimately, we chose to use the solution-phase diffusion coefficient as a reason-

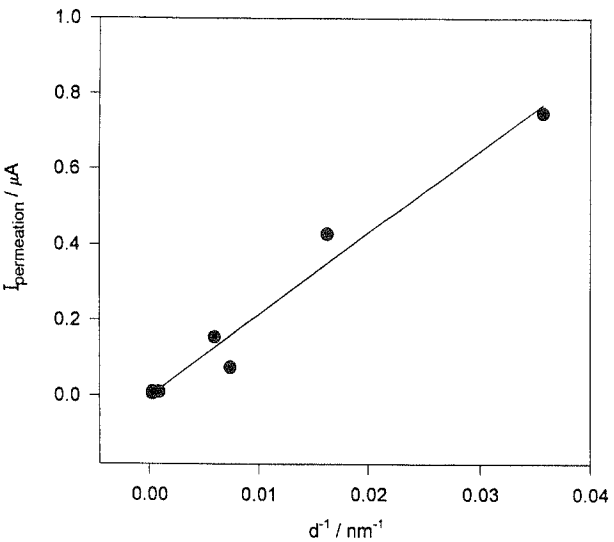

Fig. 6. Dependence of $I_{permeation}$ (Eq. (3)) for ferrocene oxidation on the reciprocal thickness d^{-1} of poly-Ru(phen)$_2$(TMP)$_2^{n+}$-based films.

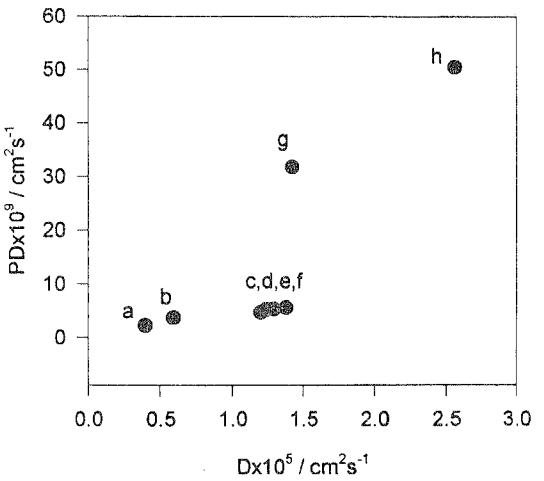

Fig. 7. Permeation rate PD_{film} versus solution phase diffusion coefficient for a series of molecular permeants (1 mM) (see caption to Fig. 2 for key). The film composition is poly-[Ru(phen)$_2$(4,4′-bpy)$_2$](ClO$_4$)$_n$. (Variable coverages, 10^{-10}–10^{-9} mol cm^{-2}.)

ably objective inverse measure of effective molecular size. (Recall that for spherical molecules, the Stokes–Einstein equation predicts an inverse relationship between D and the molecular radius. In addition, Koval et al. [17] have have established that the inverse radius relationship holds reasonably well for nonspherical molecules if geometrically averaged radii are employed.)

Fig. 7 shows a plot of permeability versus D (i.e. relative inverse molecular size (effective size)) for eight neutral permeants in a poly-Ru(phen)$_2$(4,4′-bpy)$_2^{n+}$ film. The most striking feature is the sharp cut-off of permeability with increasing permeant effective size (cf. Fig. 3). The behavior is reminiscent of prior correlations of permeability with molecular volume for vinyl(bi)pyridine-based metallopolymer films [1,3–5] and is suggestive of a relatively narrow distribution of film pore or cavity sizes. (Residual signals for the largest molecules are probably indicative of pinhole diffusion rather than true permeation.) Therefore the effective molecular size cut-off is ascribed to physical exclusion of the permeant, i.e. a drastic decrease in P. (In principle, of course, the effect also could reflect a drastic decrease in D_{film}, since only the product of P and D_{film} is measured here.)

3.4. Film structure dependence

With the behavior of intermediate linkage (i.e. 4,4′-bpy-based) films established, we sought to examine films with both longer and shorter links. Our expectation was that permeation and size-based selectivity would be modified in ways that reflected the anticipated increases and decreases respectively in polymer pore size. Fig. 8 shows plots of permeability versus D for phen-based films featuring TMP and BPEB linkages (''long linkages'', see Fig. 1). Fig. 9 presents data for films derived from Ru(Cl-phen)$_3^{2+}$ (direct linkage of phenanthroline ligands) and Fe(NH$_2$-phen)$_3^{2+}$ (probable N=N links between phen ligands) (''short linkages''). Each of the six additional films displays sharp molecular sieving behavior. Surprisingly, however, the effective molecular size cut-off (as indicated by D) is virtually the same for each film, despite calculated metal-to-metal separation distances that vary from ca. 23 Å (Ru(phen)$_2$(BPEB)$_2^{2+}$-based films) to ca. 11 Å (Ru(5-Cl-phen)$_3^{2+}$-based films)! (The cut-off occurs at a ''size'' corresponding roughly to that for 1,1′-dibenzoylferrocene or 1,1′-dimethylferrocene (see Fig. 2).)

Given the failure of fairly extensive linkage length variations to induce significant changes in molecular selectivity, we attempted to modulate selectivity by altering the metallopolymer architecture in a different way. Specifically, we attempted to diminish effective cavity volumes, for fixed linkage lengths, by introducing a phenyl substituent at the 5 site of 1,10-phenanthroline in both poly-Ru(R-phen)$_2$(4,4-bpy)$_2^{n+}$ and poly-Ru(R-phen)$_2$(TMP)$_2^{n+}$ films. The resulting permeation behavior is shown in Figs. 10 and 11. Remarkably, the phenyl-containing films display effective size selectivities that are essentially identical with those shown in Figs. 7–9.

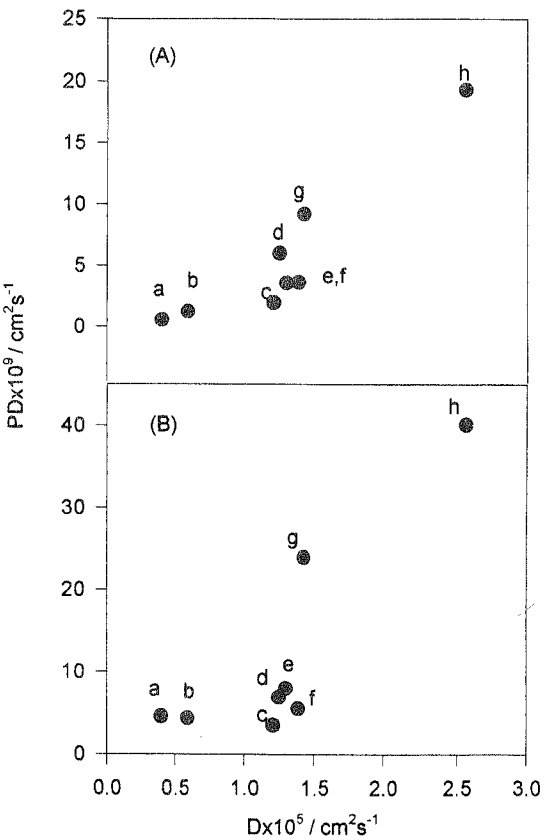

Fig. 8. Permeation rate PD_{film} versus solution phase diffusion coefficient for a series of molecular permeants (1 mM) (see caption to Fig. 2 for key) (A) poly-[Ru(phen)$_2$(TMP)$_2$](ClO$_4$)$_n$ film; (B) poly-[Ru(phen)$_2$-(BPEB)$_2$](ClO$_4$)$_n$ film. (Variable coverages, 10^{-10}–10^{-9} mol cm^{-2}.)

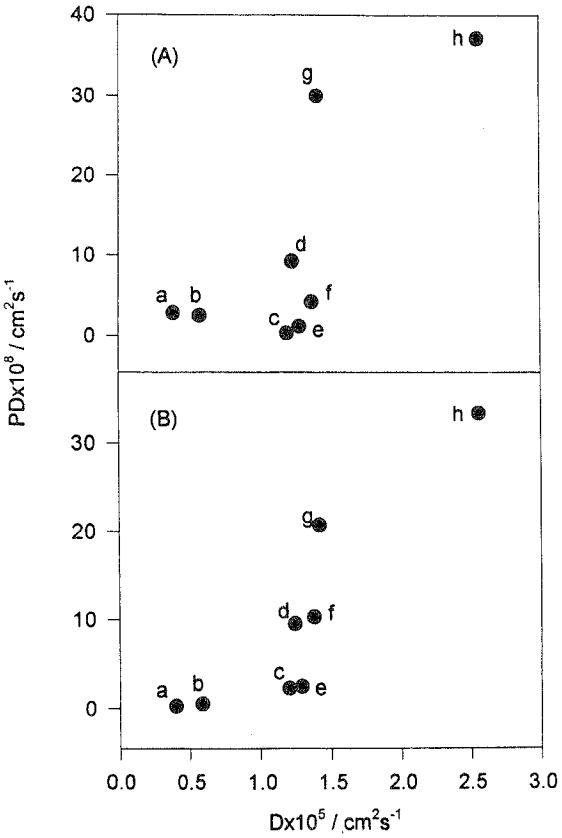

Fig. 9. Permeation rate PD_{film} versus solution phase diffusion coefficient for a series of molecular permeants (1 mM) (see caption to Fig. 2 for key): (A) film derived from $Ru(Cl\text{-}phen)_3^{2+}$; (B) film derived from $Fe(NH_2\text{-}phen)_3^{2+}$. (Variable coverages, 10^{-10}–10^{-9} mol cm^{-2}.)

The appearance of a seemingly universal polymer-based cavity or pore size, corresponding approximately to the dimensions of dimethylferrocene, is both surprising and puzzling. We speculate that the near constancy reflects a compensation between effects associated with linkage

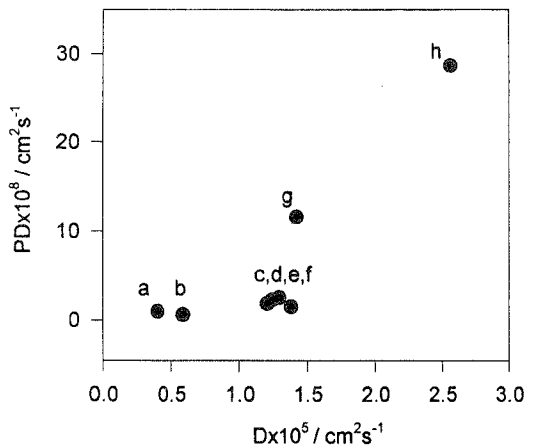

Fig. 10. Permeation rate PD_{film} versus solution phase diffusion coefficient for a series of molecular permeants (1 mM) (see caption to Fig. 2 for key). Film composition is poly-$[Ru(phenyl\text{-}phen)_2(4,4'\text{-}bpy)_2](ClO_4)_n$. (Variable coverages, 10^{-10}–10^{-9} mol cm^{-2}.)

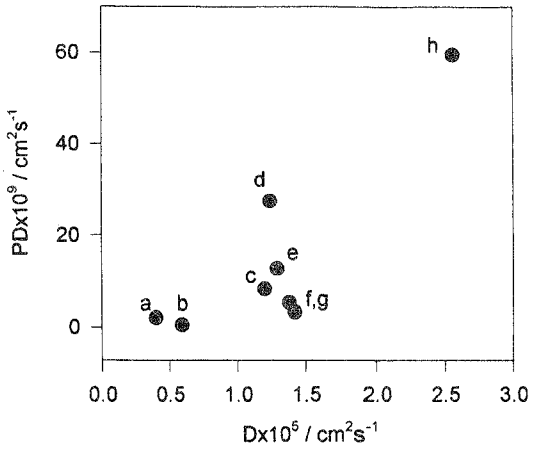

Fig. 11. Permeation rate PD_{film} versus solution phase diffusion coefficient for a series of molecular permeants (1 mM) (see caption to Fig. 2 for key). Film composition is poly-$[Ru(phenyl\text{-}phen)_2(TMP)_2](ClO_4)_n$. (Variable coverages, 10^{-10}–10^{-9} mol cm^{-2}.)

length (where longer lengths obviously should favor larger pore sizes) and degree of cross-linking (where greater cross-linking should yield smaller pore sizes). If longer linkage ligands yield significant steric advantages with respect to cross-linking efficiency, the net effect might be the observed linkage independence of the effective pore size.

Alternatively (or additionally) the constancy implied by Figs. 7–11 might be indicative of a templating effect. Film growth from cationic monomers requires intimate association with, and ultimately incorporation of, charge-compensating anions. With the possible exception of the synthesis involving $Ru(5\text{-}Cl\text{-}phen)_3^{2+}$ (where chloride ions may be incorporated [13]), film growth requires participation specifically of the electrolyte-based perchlorate ions. Presumably the anion imposes a minimum pore/cavity size corresponding approximately to its diameter (ca. 4.2 Å) or volume (ca. 39 Å^3). For comparison, the approximate diameter of ferrocene is 4.8 Å (major axis), and the approximate van der Waals volume is 68 Å^3.

If the second explanation is correct (or partially correct), it suggests that the initial goal of controlling permeant selectivity by manipulating effective metallopolymer pore sizes might be achievable by varying the electrolyte anion size [18]. Alternatively, a (secondary) cross-linking reaction after film formation [19] might provide a viable route to cavity/pore-size modulation and varied permeant selectivity.

Yet another possibility is that films are not swollen by acetonitrile, i.e. that the cavities collapse. Pore sizes would then be defined primarily by monomer sizes (approximately constant; however, note Figs. 10 and 11), rather than linkage lengths (widely varying). However, this explanation would be likely to be fully applicable only to those polymers featuring flexible linkages.

4. Conclusions

Metallopolymeric films featuring widely varying metal-to-metal linkage lengths can be prepared via a combination of oxidative and reductive electropolymerization schemes. All the films exhibit size selective permeability behavior towards molecular reactants. Surprisingly, however, the molecular size cut-off is independent of film composition, implying that films with widely varying metal-to-metal linkage lengths nevertheless contain pores of very similar size. Attempts to diminish effective pore sizes by introducing large ligand substituents (phenyl groups) at the monomer synthesis stage were unsuccessful, at least as judged by subsequent film permeation studies. We speculate that the potential pore-size expansion effects expected from linkage length extension are compensated by enhanced cross-linking. Alternatively (or additionally), the near constancy of effective pore sizes may be indicative of an electrolyte anion templating effect during film formation.

Acknowledgements

SGY thanks Dr. Dong Yoon for advice on the synthesis of BPEB. We thank Lora L. Nugent (Pew Foundation Summer Undergraduate Fellow) and Daniel Sauri (MRC Summer Undergraduate Fellow) for carrying out preliminary permeation measurements on some of the metallopolymeric films. We thank the NSF Materials Research Center at Northwestern (DMR-9120521) and the Office of Naval Research for support of this work. JTH gratefully acknowledges a Teacher-Scholar Award (1991–96) from the Dreyfus Foundation.

References

[1] S. Gould and T.J. Meyer, J. Am. Chem. Soc., 113 (1991) 7442.
[2] T. Ohsaka, T. Hirokawa, H. Miyamoto and N. Oyama, Anal. Chem., 59 (1987) 1758.
[3] A.G. Ewing, B.J. Feldman and R.W. Murray, J. Phys. Chem., 89 (1985) 1263.
[4] T. Ikeda, R. Schmehl, P. Denisevich, K. Willman and R.W. Murray, J. Am. Chem. Soc., 104 (1982) 2683.
[5] S. Gould, G.F. Strouse, T.J. Meyer and B.P. Sullivan, Inorg. Chem., 30 (1991) 2942.
[6] K.A. Pressprich, S.G. Maybury, R.E. Thomas, R.W. Linton, E.A. Irene and R.W. Murray, J. Phys. Chem., 93 (1989) 5568.
[7] R. Pyati and R.W. Murray, J. Phys. Chem., 93 (1989) 5568.
[8] O. Fussa-Rydel and J.T. Hupp, J. Electroanal. Chem., 251 (1988) 417.
[9] H.T. Zhang, P. Subramanian, O. Fussa-Rydel, J.C. Bebel and J.T. Hupp, Solar Energy Mater. Solar Cells, 25 (1992) 315.
[10] J.M. Calvert, D.L. Peebles and R.J. Nowak, Inorg. Chem., 24 (1985) 3111.
[11] L. Skeens-Jones, J.A. Ibers, P. Subramanian and J.T. Hupp, unpublished studies.
[12] C.D. Ellis, L.D. Margerum, R.W. Murray and T.J. Meyer, Inorg. Chem., 22 (1989) 1283.
[13] O. Fussa-Rydel, H.T. Zhang, J.T. Hupp and C.R. Leidner, Inorg. Chem., 28 (1989) 1533.
[14] H.D. Abruna, A.I. Breikss and D.B. Collum, Inorg. Chem., 24 (1985) 987.
[15] A.A. Schilt, J. Am. Chem. Soc., 82 (1960) 3000.
[16] J.M. Calvert, R.H. Schmehl, B.P. Sullivan, J.S. Facci, T.J. Meyer and R.W. Murray, Inorg. Chem., 22 (1983) 2151.
[17] C.A. Koval, M.E. Ketterer and C.M. Reidsema, J. Phys. Chem., 90 (1985) 4201.
[18] S. Cosnier, A. Deronzier and J.-F. Roland, J. Electroanal. Chem., 310 (1991) 71.
[19] R.L. McCarley, R.E. Thomas, E.A. Irene and R.W. Murray, J. Electroanal. Chem., 290 (1990) 79.